Building Reduced Model for MILP Optimization: Application to Demand Response of Residential Buildings

Camille Pajot, Nils Artiges, Benoît Delinchant, Yves Maréchal

Building Reduced Model for MILP Optimization: Application to Demand Response of Residential Buildings

Camille Pajot[1], Nils Artiges[1], Benoit Delinchant[1], Yves Marechal[1]
[1]Univ. Grenoble Alpes, CNRS, Grenoble INP, G2Elab, 38000 Grenoble, France

Abstract

This paper addresses the topic of the electrical flexibility on the demand-side, by focusing on the residential buildings. Specifically, it aims to quickly formulate the optimal operation of building heat pumps, according to environmental or grid issues. Indeed the literature shows many examples of quantification of the flexibility impacts, but mostly relying on predefined strategies. To go from the evaluation of some strategies to the formulation of the optimal planning, we are introducing a methodology based on the automatic generation of models dedicated to mixed-integer linear programming (MILP) optimization. Finally, the method was applied to a new residential building during a month of winter.

Introduction

Flexibility context on the electrical system

According to the Intergovernmental Panel on Climate Change (2018), climate-related risks to health, livelihoods, food security, water supply, human security, and economic growth are projected to increase with global warming. Limiting global warming to 1,5 °C requires the energy system to undergo a rapid transition. One solution to reduce the CO_2 emitted by the energy system is to increase the share of renewable energies into the energy production mix. As a massive integration of variable renewable energies in the power system could lead to stability issues, flexibility becomes key to the energy transition (IRENA (2018)). In order to increase the flexibility means on the electrical system, the consumption site has been involved through the concept of Demand-Side Management (Meyabadi and Deihimi (2017)).

According to the International Energy Agency (2018), the global buildings sector accounts for more than 55% of global electricity demand, so that they represent a massive and diffuse electricity consumption. Besides electrical appliances, the electricity can be converted into heat in order to cover the thermal needs. This possibility of conversion from electricity to heat is usually called Power-to-Heat (P2H) and allows the use of the flexibility on a thermal load for electrical grid purposes (Bloess et al. (2018)). As buildings can store heat into their own envelope thanks to thermal inertia, P2H can be applied to buildings equipped with heat pumps, electric heaters or even electric boilers.

Approaches for DSM modeling

In order to quantify the impacts of a DSM (Demand Side Management) strategy, load forecast models are required. In the particular case of using heat pumps flexibility, the load to be predicted corresponds to the thermal needs of the building. The literature mostly shows two approaches for heat load forecasting:

1. Data-driven models
2. Physical models

In the first case, the load predictions rely on historical data, on which various machine learning methods (from linear regression to neural networks) are applied for the future load forecast (Yildiz et al. (2017), Amasyali and El-Gohary (2018)). In order to be successful, these methods require a large amount of data. Indeed, in order to provide efficient hours-ahead building load forecasts, Ke et al. (2016) used 15-minutes building load data from May 2012 to April 2014. Similarly, Bacher et al. (2013) used measurements over a two-year period with a 10-minute time step. When as many data are not available, an alternative to these "black box" models is to exploit the laws of physics for thermal transfers, also called "white box" or "grey box" (Harish and Kumar (2016)). Besides solving a data issue, using physical laws can lead to greater reliability of the load forecast.

A large range of physical models can be found in the literature, from very-detailed to low-level models (Reinhart and Davila (2016)). Very-detailed models are generally based on the thermal zone concept, which considers parts of the building with a homogeneous temperature as a single "thermal zone" and decomposed buildings elements such as walls with a finite volume method (Peuportier and Blanc (1990)). Software with detailed thermal models, including all the thermal zones and the energy systems are used for regulation purposes, such as guarantee-

ing the respect of the maximal energy consumption of a building during the design phase (Allegrini et al. (2015)). In the opposite, thermal models such as Resistance-Capacitance (RC) networks applied to an entire building can significantly reduce the simulation time of the thermal load forecasting model. Therefore, when scaling up from building to the district, RC networks tend to be preferred (Elci et al. (2018)). Another alternative is available to gain time during the design of the study case: model generation tools. By using standard languages, these tools have the main advantage to provide reusable models. For instance, Remmen et al. (2018) provide TEASER (Tool for Energy Analysis and Simulation for Efficient Retrofit) for the creation of building models in the Modelica language.

Once the consumption models created, the strategies of demand-side management can be applied and evaluated. The performance of a strategy can be quantified by introducing evaluation indicators, such as the CO_2 emissions, the operative temperature or peak shaving. However, in the case of simulation models, each strategy should be pre-defined, then tested and evaluated afterward, so that a simulation-based approach cannot provide new solutions. To go further in the formulation of DSM scenarios according to its purposes, optimization is thus needed. For this reason, this paper aims to develop a methodology to define optimal operation strategies of a building heat pump.

Paper structure

First, the methodology implemented to quickly generate optimization models for DSM on buildings heating loads will be presented. Then, the methods will be applied to a residential building, aiming either to minimize its electric peak power or its CO_2 emissions. In the results section, the optimization results obtained on the study case will be presented. Finally, after a discussion section, a conclusion will be drawn.

Methods

Quick generation of optimization models

The paper aims to provide a method to quickly determine optimal heat pumps operation strategies. Optimization allows finding the best DSM strategy according to criteria, instead of testing several predefined strategies in simulation and evaluating the impact afterward. For this purpose, a first requirement is heating loads models suited for optimization. Then, the generation of these models has to be fast and replicable. To do so, we rely on the OMEGAlpes open source software[1], which allows a quick design of optimization problems. The models are generated into a Mixed-Integer Linear Programming (MILP) formulation in order to quickly provide a solution with a large number of variables. Thus, the thermal load model has to respect this linear formulation. This is a key point that we are addressing in this paper, and especially for non-linearities occurring in radiative exchanges.

[1] https://gricad-gitlab.univ-grenoble-alpes.fr/omegalpes

Thermal load forecast

The district scale can be very different from the building scale by the number of stakeholders involved in the energy decisions, and thus by the availability of relevant data. Indeed, consumption data are much easier to get for study cases at a building scale, than for an entire district. This poor data access when scaling up to the district scale needs to be taken into consideration. Thus, data-driven load forecast methods can be difficult to apply to an entire district. Moreover, a thermal load is much more correlated to data such as the external temperature for low-insulated buildings than for the new high-efficiency ones. Therefore, this paper only focuses on a physical modeling approach.

However, as they require a large amount of specific data on each building, very-detailed models are out of scope too. Besides not being available, a very large amount of data could lead to computational issues during the resolution of the optimization problem. Therefore, reduced models are wished for the optimization model of the heating load prediction, as soon the level of modeling is effective enough to describe buildings responses to DSM events.

Low-level RC networks could fit the requirements since their utilization in order to simulate the impact of DSM strategies on building heating loads was validated in a previous study (Pajot et al. (2018)). Moreover, the model has to be linear in order to fit with the linear formulation of the optimization problem (MILP). As there are many variants of these models, this study focus on the RC model used for regulatory studies in both the French and Swiss contexts (RT2012 and SIA 2044) and drawn in Figure 1. The model described in Figure 1 is related to SIA 2044 and was extracted from the framework City Energy Analyst from ETH Zurich (Fonseca et al. (2016)).

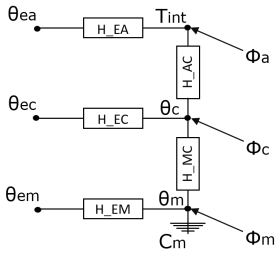

Figure 1: Resistance-Capacitance network model

Six nodes of temperature are linked by five thermal resistances and one capacitance. The three nodes on the left of the thermal model are related to external temperatures, while the right part describes internal behaviours.

Then, the top represents the ventilation, through an

heat flow rates (Φ_{vent}) between the ambient air (T_{int}) and the injected air (θ_{ea}), according to :

$$\Phi_{vent} = H_{EA}(T_{int} - \theta_{ea}) \tag{1}$$

The bottom part represents the heat exchanges at the building mass. The temperature at its internal surfaces is expressed by θ_m, while θ_{em} stands for its external surfaces. Thus, the transmission losses with outside (Φ^m_{trans}) can be expressed by the expression (2). Moreover, an internal heat capacity (C_m) is connected to the node (m), since the main source of heat storage in a building corresponds to its mass.

Finally, the light surfaces of the building, such as the windows, are integrated into the node (c). This node reflects an average behavior between theses surfaces, the building mass and the ambient air. The transmission losses occurring at light surfaces are thus considered by Φ^c_{trans}, as expressed in (2).

$$\begin{cases} \Phi^c_{trans} = H_{EC}(\theta_c - \theta_{ec}) \\ \Phi^m_{trans} = H_{EM}(\theta_m - \theta_{em}) \end{cases} \tag{2}$$

However, theses losses can be compensated by heat gains, from solar radiation, but also occupancy, appliances and lighting. All the gains from inside or outside can be split between the three internal nodes of temperature (T_{int}, θ_c and θ_m) and are respectively called Φ_a, Φ_c and Φ_m, as shown Figure 1. Splitting the internal gain between the nodes was realized with coefficients whose values were extracted from the Swiss norm SIA 2044, according to the calculations found in Fonseca et al. (2016). Therefore, the heat flow rates from lightning (Φ_{il}), occupancy (Φ_{ip}) and appliances (Φ_{ia}) are distributed according to (3) to form the internal gains.

$$\begin{cases} \Phi^{int}_a = (1 - f_{rl})\Phi_{il} + (1 - f_{rp})\Phi_{ip} + (1 - f_{ra})\Phi_{ia} \\ \Phi^{int}_{\substack{c \\ m}} = f_{\substack{c \\ im}}(f_{rl}\Phi_{il} + f_{rp}\Phi_{ip} + f_{ra}\Phi_{ia}) \end{cases} \tag{3}$$

The external gains (Φ_s) are split between the nodes of temperature (a, c and m), as follows (4):

$$\begin{cases} \Phi^{ext}_a = f_{sa}\Phi_s \\ \Phi^{ext}_{\substack{c \\ m}} = (1 - f_{sa})f_{\substack{s \\ sm}}\Phi_s \end{cases} \tag{4}$$

Finally, the heat flow rate corresponding to the heating and cooling systems (Φ_{hc}) can be applied to the nodes. The radiative fraction ($\Phi_{hc,r}$) is applied to the nodes relating to c and m (5).

$$\Phi_{\substack{c \\ m}} = \Phi^{int}_{\substack{c \\ m}} + \Phi^{ext}_{\substack{c \\ m}} + f_{\substack{c \\ im}}\Phi_{hr,r} \tag{5}$$

For the ambient air, the convective fraction of the heat flow rates from heating and cooling ($\Phi_{hc,cv}$) is added to the internal and external flows (6).

$$\Phi_a = \Phi^{int}_a + \Phi^{ext}_a + \Phi_{hr,cv} \tag{6}$$

The external gains (Φ_s) can be split into the net solar radiation to the building (I_{sol}) and heat flow rates the re-irradiated to the sky (I_{rad}).

$$\Phi_s = I_{sol} - I_{rad} \tag{7}$$

Both the incident and the re-irradiated heat flow rates can be divided between the walls, the windows and the roof (8 and 14). The incident solar gains to the building depend on the average value of the solar radiation (8).

$$I_{sol} = I^{av}_{sol}(\gamma_{win} + \gamma_{wall} + \gamma_{roof}) \tag{8}$$

Where:

$$\begin{cases} \gamma_{win} = A_{win} * (1 - F_F) * Fsh_{win} \\ \gamma_{wall} = A_{wall} * R_{SE} * a_{wall} * U_{wall} \\ \gamma_{roof} = A_{roof} * R_{SE} * a_{roof} * U_{roof} \end{cases} \tag{9}$$

Despite benefiting from solar radiation, buildings are continuously exposed to the sky, so that radiative exchanges occur between buildings elements (windows, walls and roof) and the sky. For each element x, this re-irradiated heat flow to the sky, which is non-linear regarding surface temperature (θ_c), can be expressed as (10) and is usually found under the form (11) in building physics applications.

$$I_{rad,x} = \epsilon_x * \sigma * A^c_x * (T^4_{sky} - \theta^4_c) \tag{10}$$

$$I_{rad,x} = \underbrace{\epsilon_x \sigma (T^2_{sky} + \theta^2_c)(T_{sky} + \theta_c)}_{h_{rad,x}} * A^c_x * (T_{sky} - \theta_c) \tag{11}$$

Where ϵ_x is the emissivity of the element x, σ the Stefan-Boltzmann constant, T_{sky} the temperature of the sky, θ_c the temperature defined previously, $h_{rad,x}$ is an external radiative heat transfer coefficient for the element x and A^c_x is its effective solar collecting area (12) according to the norm ISO 13790 (2008):

$$A^c_x = F_{f,x} * R_{SE} * U_x * A_x \tag{12}$$

Where R_{SE} is the external surface heat resistance of the opaque part, $F_{f,x}$ is the form factor of the element x (0,5 for vertical surfaces and 1 for horizontal surfaces), U_x is the thermal transmittance of the element x and A_x is its surface.

In buildings physic literature, numerous simplifications are realized for the expression of the external radiation heat transfer coefficients ($h_{rad,x}$) from empirical values (around $5 W/m^2K$) to more complex calculation depending on the wind speed (Evangelisti et al. (2017)). The Standard UNI EN ISO 6946 recommends to express $h_{rad,x}$ as follows (13).

$$h_{rad,x} = 4 * \epsilon_x * \sigma * (\frac{T^t_{sky} + \theta^{t-1}_c}{2})^3 \tag{13}$$

Therefore the re-irradiated heat flow can be expressed by a polynomial of θ_c^{t-1} and T_{sky}^t (14).

$$\begin{cases} I_{rad} = p(\theta_c^{t-1}, T_{sky}^t)(k_{win} + k_{wall} + k_{roof}) \\ p(x,y) = (y-x)(x+y)^3 \end{cases} \quad (14)$$

Where:

$$\begin{cases} k_{win} = F_{f,win} * R_{SE} * U_{win} * A_{win} * \epsilon_{win} * \sigma/2 \\ k_{wall} = F_{f,wall} * R_{SE} * U_{wall} * A_{wall} * \epsilon_{wall} * \sigma/2 \\ k_{roof} = F_{f,roof} * R_{SE} * U_{roof} * A_{roof} * \epsilon_{roof} * \sigma/2 \end{cases} \quad (15)$$

In the case of Dynamic Thermal Simulation (DTS), the resolution of the previous equations (or variants) is realized once per time step. However, in order to be integrated into an optimization approach, specific requirements need to be considered.

Optimization requirements

In opposite to DTS models, the optimization model has to integrate all the time steps simultaneously to find the optimal operation of the heating system. Thus, no iterative process can be incorporated into the MILP formulation of the study case, which represents a big difference with the simulation models.

Besides considering the time-dependency when it is the case, all the equations should be acausal. Thus, all the dynamic variables calculated at each iteration of the simulation become as many decisions variables as the number of time steps and differential equations can be written as difference equations. This way, all equations from the simulation model can be converted into optimization ones and expressed as optimization constraints.

Moreover, the constraints expressed in a MILP model can only be described as linear expressions of the decision variables. However, the Stefan-Boltzmann law expressed in (14) is non-linear and cannot be integrated as such in the MILP model. Indeed, the θ_c value is calculated at each iteration during the simulation process and therefore is a decision variable in the optimization model. In order to be considered, this heat flow rate has to be linearized. In the case of a MILP formulation, one solution is to introduce new constraints with binary variables. Nevertheless, this method could lead to computational issues when the expression to be linearized is time-dependent. More traditional approaches include using Taylor development (16) to express the function around a point of interest (x_l) or several ones through a piecewise linear function.

$$f(x) \simeq \sum_{i=0}^{n} \frac{f^{(i)}(x_l)}{i!}(x - x_l)^i \quad (16)$$

Since the temperature of the sky (T_{sky}) only depends on weather data and is entirely known out of the optimization, the expression of the re-irradiated heat flow has to be linearized only with respect to θ_c.

The range of variation of θ_c is relatively small as the temperature of the surfaces is quite close to the mean ambient temperature of a temperature-regulated building. For this reason, an estimation of the mean temperature of the thermal zone (T_{mean}) is chosen as the point of interest in the linearization, so that I_{rad} can be expressed as (17).

$$I_{rad}(\theta_c^{t-1}) \simeq \sum_{i=0}^{n} \frac{I_{rad}^{t(i)}(T_{mean})}{i!}(\theta_c^{t-1} - T_{mean})^i \quad (17)$$

A first approach consist in assuming θ_c to be constant, i.e. considering the Taylor formula (17) at the order 0. Then, a second step is realized with a development at the first order. The two methods are illustrated in Figure 2 and will be developed in the next subsection.

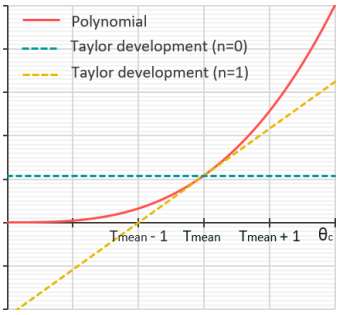

Figure 2: Illustration of the linearization method

Linearization results

As explained previously, the MILP formulation of the optimization problem requires all equations to be linear in order to be set as constraints. As I_{rad} can be expressed as a fourth-degree polynomial of θ_c (14), two linearization methods were presented:

1. The first linearization considered a fixed value of θ_c equals to T_{mean} ((17) at order 0).
2. The second method assumed a linear variation of I_{rad} depending on θ_c ((17) at order 1).

Dynamic results of these linearizations are shown in Figure 3 on a 48-hour period, with a time step of 10 minutes. For reference, the real calculation of I_{rad} is represented by a blue line, while the orange and green bullets respectively stand for the first and second method.

First, it can be noticed that results obtained by the first method change per stages. This can be explained by the time steps of the data. As the external temperature is hourly predicted, the sky temperature is calculated with an hourly time step. As the value of θ_c^{t-1} in the method is set to T_{mean} $\forall$ t, the estimation of I_{rad}^t only fluctuate according to T_{sky}^t. In the other hand, the orange curve representing the second linearization method fits all variations with a good approximation.

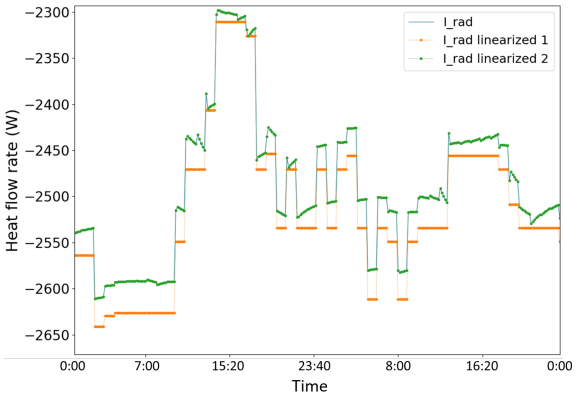

Figure 3: Comparison between I_{rad} and I_{rad} linearized (two ways) during 48 hours

The mean absolute error (18) obtained during a month of winter with T_{mean} set to T_{set} = 19°C is 0,89% for the first method and 0,0013% for the second method.

$$\text{Error} = \frac{1}{\text{period length}} * \sum_{period} \frac{\mid \hat{I}^t_{rad} - I^t_{rad} \mid}{\mid \hat{I}^t_{rad} \mid} \quad (18)$$

In these cases, the approximation of the mean value of θ_c (19°C) is very close to the real mean temperature (18,9°C). However, this method was applied to a thermally controlled building, so that the mean temperature of the surfaces is not supposed to vary much. In cases of non-controlled buildings or during load shedding strategies, higher variations of temperature may occur on the surfaces. Therefore, the prediction was realized again with an estimation of T_{mean} with variations of +/- 1°C and +/- 4°C, with the same real mean temperature. The results are shown in Table 1.

T_{mean}	Error - lin. 1	Error - lin. 2
15°C	15 %	0,30 %
18°C	3,3 %	0,014 %
19°C	0,89 %	0,0013 %
20°C	4,8 %	0,028 %
23°C	17 %	0,35 %

Table 1: Mean error of estimation of I_{rad} according to T_{mean}

Even with a supposed mean temperature of surfaces 4°C lower or higher than the right one, the second method estimates I_{rad} more accurately than the estimation realized with the first method with 19°C. For this reason, the estimation of I_{rad} provided by the second method (Taylor development at the first order) was integrated into the optimization model for the prediction of the thermal needs.

Application to a residential building

In order to find the best operation of the heat pump in a residential neighborhood, the desired objectives for the DSM have to be defined. In this paper, two objectives have been studied:

1. Minimizing the CO_2 emissions
2. Minimizing the peak consumption power

For an eco-district, lowering its environmental impact is very important, so that minimizing the CO_2 emissions related to the heating consumption of the buildings may be more and more investigated. However, the CO_2 emissions generated for the production of a kilowatt-hour is time-dependent, according to the production mix needed to match the consumption. Shifting electrical loads to low-pollution periods can easily be realized in case of a building thermally fed by heat pumps and will be explored in this paper.

The CO_2 emissions are calculated from the consumption of the heat pump, according to the hourly emission of the French electrical system (19).

$$CO_2\text{em.} = \frac{1}{COP_{HP}} \sum_{January} co_2^t * \Phi_{hc}^t \quad (19)$$

The CO_2 emissions of the French electrical system (co_2^t) are taken during the year 2017, while the power needs (Φ_{hc}^t) result from the optimal strategy. In this case, the heat provided to the heat pumps comes from ground water whose temperature can be considered as constant, so that COP_{HP} too.

Then, a more local point of view was adopted with the minimization of the peak consumption power. Peak shaving strategies can be crucial for distribution system operators, as they can avoid congestion on the power lines and reduce the risk of instability on the entire power system. For this reason, the second objective studied in this paper is the minimization of the peak consumption power required for the building heating needs.

From an electric point of view, the time of the year when the grid is the most at risk in France is the winter. For this reason, both of these objectives will be applied for the month of January. During this period, the dynamic was modeled with a time step of 10 minutes. Moreover, to ensure simplicity in the formulation, this paper focuses on the operation of the heat pump of a single building of the block.

As an optimal operation of the heat pump could affect the thermal comfort of the building occupants, a specific constraint has been defined. In order to express the thermal comfort, this paper relies on the operative temperature calculated as the mean value between the temperatures representing the radiative and the convective heat flows for the occupants, according to the approximation defined by ASHRAE (2013). With the definition of θ_c, the norm calculates $T_{operative}$ as follows (20):

$$T_{operative} = 0,69 * \theta_c + 0,31 * T_{int} \quad (20)$$

The constraint ensures that the operative temperature, stays between +/- 1 °C around the temperature set-point.

Then, all the external and internal flows are required in order to build the thermal model. Internal flows

are usually estimated thanks to occupancy prediction (see Figure 4), while the external heat flow rates rely on weather data.

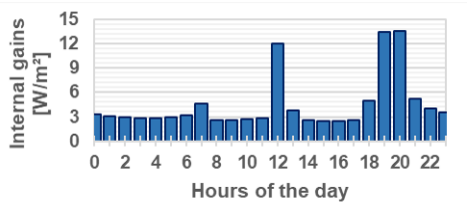

Figure 4: Internal heat flow rates per area

In this study, representative weather files for the location were found online (EnergyPlus (2018)) and extracted for the month of January.

Data relative to the building were obtained from mandatory studies for the construction of new residential buildings. An occupancy schedule was realized and provides us the internal gains of the building per surface (Figure 4).

Standard data about the envelope of the building were also available and the most important parameters (U-values, areas, emissivity: ϵ and absorptivity: α) are summarized in Table 2.

Table 2: Envelope data of the building

	U [W/(m^{2}K)]	**A [m^2]**	ϵ	α
Windows	1.1	520	0.9	
Walls	0.18	1990	0.9	0.6
Roof	0.12	263	0.9	0.5

Once the model built, three optimization problems were launched: a reference scenario, the minimization of the CO_2 emissions and the minimization of the maximal peak power. For comparison, the operation for reference scenario corresponds to the heating supply providing the least variation of the operative temperature around its set-point.

Results

In this section, the results for optimal operation of the heat pump of a new residential building during January are detailed. First two mono-objective approach are investigated in order to study both the environmental and financial objectives. Then, the results from a multi-objectives study are presented to find some trade-offs between these points of view.

Mono-objective optimizations

As explained before, a reference scenario was defined as the heat pump operation needed to lower the gap between the operative temperature and its set-point. Then, two optimal scenarios respectively minimizing the consumption peak and the CO_2 emissions have been studied through a MILP formulation.

With 93745 variables (80353 continuous and 13392 binary) and 271859 non-zeros, this optimization problem was solved within 32 seconds with the Gurobi solver on an Intel bicore i5 2.4 GHz CPU. The results obtained from the three operation strategies can be found in Table 3, in terms of electrical peak power (p^{elec}_{peak}), CO_2 emissions (CO_2 em.), electrical consumption (Elec cons.) and mean operative temperature (T^{op}_{mean}). For comparison to other buildings, it can be added that the considered building includes an area of 3436m^2 heated by a heat pump with a coefficient of performance equals to 4.

Table 3: Optimization results

	Ref.	**Obj. peak**	**Obj. CO_2**
P^{elec}_{peak}	50,0 kW	4,41 kW	16,7 kW
CO_2 em.	173 kg	98,6 kg	82,0 kg
Elec cons.	12 MWh	6,9 MWh	5,8 MWh
T^{op}_{mean}	19,0 °C	19,1 °C	18,7 °C

As we can see, the reference scenario is the worst from three points of views (the emissions of CO_2, the electrical peak power and electrical consumption). Even from the operative temperature perspective, 0,1 °C more on average are obtained by minimizing the peak power.

For this first objective, the heat pump operation allows dividing the peak power by 11 (91% of diminution), while reducing both the CO_2 emissions and the energy consumption, from 43%. In order to reach a reduction of the CO_2 emissions from 53% with the second optimization, the power peak decreases from 67% and the energy consumption is lowered with 52%.

In both cases, the energy consumption decreases as much as CO_2 emissions, which suggests that reducing the energy consumption could lead to a similar reduction of the CO_2 emissions.

Multi-objectives optimization

In order to find trade-offs between the two points of views, study cases with weighted objectives have been realized and are shown on a Pareto diagram (Figure 5). Thus, several possibilities can be found allowing stakeholders to choose the better compromise according to them, between peak shaving and the desire of minimizing the CO_2 emissions. These trade-off scenarios can be found in the bottom-left area of the Figure 5, where increasing the peak allows to consumed more during low-CO_2 periods and vice-versa.

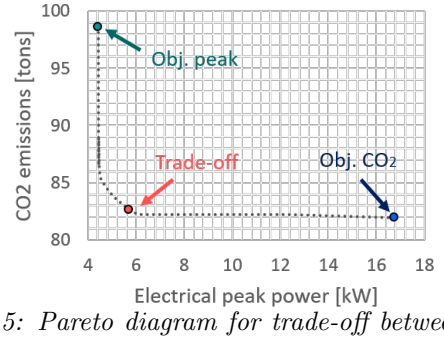

Figure 5: Pareto diagram for trade-off between CO_2 emissions reduction and electrical peak shaving

Finally, a specific trade-off providing an electrical peak power of 5,70 kW, while emitting 82,7 kg of CO_2 was selected (see Figure 5). The heat pump operation is drawn Figure 6 in line with the dynamic CO_2 emissions from the French electrical system (during 2017) and the operative temperature of the building, which must remain between 18 °C and 20 °C.

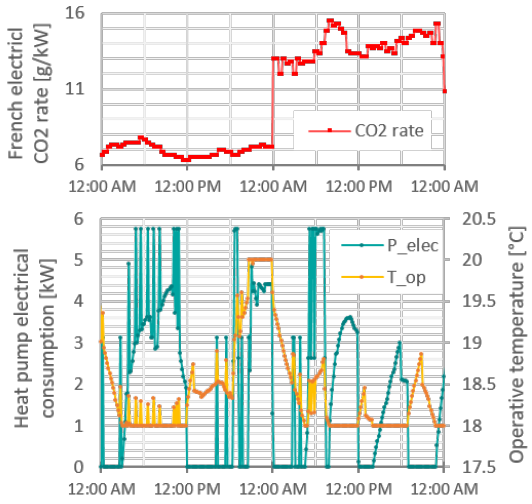

Figure 6: Heat pump operation for the selected trade-off according to CO_2 rate and operative temperature

It can be noticed that the heat pump is operating preferably during the low-CO_2 emissions periods while being constrained by the operative temperature range to maintain. By considering a trade-off instead of the solution of minimizing the CO_2 emissions, the power peaks during low-CO_2 periods are limited to 5,70 kW, instead of 16,7kW.

Conclusion and perspectives

Conclusion

In this paper, two main subjects have been developed.

A generic methodology for quick generation of MILP optimization models for DSM on buildings heating loads at the district scale, suitable for any building type. A low-level RC model dedicated for thermal dynamic simulation was converted into a MILP optimization model, by applying two linearization methods of the heat flow rate re-irradiated to the sky (I_{rad}). Providing the best estimation, the second method, based on a Taylor development at the first order, was kept for an illustration on the study case.

The application of the optimization models on a new residential building, in order to find the best operation of the heat pump according to two criteria: the CO_2 emissions and the peak power. First, the two objectives have been studied separately and compared to a reference scenario. Then, combining the two point of views was investigated by weighting the objectives. These results were shown in a Pareto diagram and a trade-off was selected for further studies. Finally, dynamic results of the heat pump operation were presented for a 48-hour period.

Perspectives

As explained previously, this work was based on a low-level RC-model, with one capacitance. As these elements represent the thermal storage capacity of the building, further work is needed to confirm the accuracy of the results. To do so, this approach could be confronted with the results obtained with a highly-detailed simulation model, by applying the optimal strategies obtained and evaluate the same indicators (power peak, CO_2 emissions, electrical consumption and mean operative temperature).

Another perspective is to extend this methodology to the entire block of buildings. This step only requires the envelope data from the buildings (U-values, areas, emissivity, and absorptivity of the walls and windows), as well as the internal gains.

Acknowledgment

This work has been partially supported by the ANR project ANR-15-IDEX-02.

Nomenclature

A_x:	Area of the element x
A_x^c:	Effective solar collecting area of x
C_m:	Internal heat capacity
co_2^t:	CO_2 emissions of a French electrical kWh at time t (during 2017)
$CO_{2,em}$:	Total CO_2 emissions
COP_{HP}:	Heat pump coefficient of performance
ϵ_x:	Emissivity of the element x
F_F:	Frame area faction coefficient
$F_{f,x}$:	Form factor of the element x
f_{im}^c:	SIA 2044 internal coefficient for the node c/m
f_{ra}:	SIA 2044 coefficient for appliances
f_{rl}:	SIA 2044 coefficient for lightning
f_{rp}:	SIA 2044 coefficient for occupancy
f_{sa}:	SIA 2044 coefficient for the node a
f_{sm}^c:	SIA 2044 external coefficient for the node c/m
$h_{rad,x}$:	External radiative heat transfer coefficient for the element x
H_{XY}:	Thermal transmission coefficient between the nodes X and Y
$\hat{I}_{rad}$:	Estimation of the heat flow rate re-irradiated to the sky
I_{rad}:	Heat flow rate re-irradiated to the sky
$I_{rad,x}$:	Heat flow rate re-irradiated to the sky from the element x
I_{sol}:	Net solar radiation to the building
I_{sol}^{av}:	Average value of the net solar radiation to the building
Φ_a:	Heat flow rate at the node a
Φ_a^{ext}:	External heat flow rate at the node a
Φ_a^{int}:	Internal heat flow rate at the node a
Φ_c:	Heat flow rate at the node c
Φ_m:	Heat flow rate at the node m

$\Phi^{ext}_{\substack{c \\ m}}$:	External heat flow rate at the node c/m
$\Phi^{int}_{\substack{c \\ m}}$:	Internal heat flow rate at the node c/m
Φ_{hc}:	Building heating/cooling power
$\Phi_{hc,cv}$:	Convective part of heating/cooling
$\Phi_{hc,r}$:	Radiative part of heating/cooling
Φ_{ia}:	Internal gains from appliances
Φ_{il}:	Internal gains from lightning
Φ_{ip}:	Internal gains from occupancy
Φ^{k}_{trans}:	Heat flow rate due to transmission through the envelope at the node k
Φ_{s}:	External heat gains
Φ_{vent}:	Heat flow rate due to ventilation
R_{SE}:	Thermal resistance of external surfaces according to ISO 6946
σ:	Stefan-Boltzmann constant
θ_{ea}:	Temperature at the node ea [°C]
θ_{ec}:	Temperature at the node ec [°C]
θ_{em}:	Temperature at the node em [°C]
θ_{c}:	Temperature at the surfaces [°C]
θ_{m}:	Temperature at the thermal mass [°C]
T_{int}:	Temperature of the ambient air [°C]
T_{mean}:	Estimation of the mean temperature of the surfaces [°C]
$T_{operative}$:	Operative temperature of the zone
T_{sky}:	Temperature of the sky [K]
U_{x}:	Thermal transmittance of x

References

Allegrini, J., K. Orehounig, G. Mavromatidis, F. Ruesch, V. Dorer, and R. Evins (2015). A review of modelling approaches and tools for the simulation of district-scale energy systems. *Renewable and Sustainable Energy Reviews 52*, 1391 – 1404.

Amasyali, K. and N. M. El-Gohary (2018). A review of data-driven building energy consumption prediction studies. *Renewable and Sustainable Energy Reviews 81*, 1192 – 1205.

ASHRAE (2013). ANSI/ASHRAE Standard 55-2010. pp. 44.

Bacher, P., H. Madsen, H. A. Nielsen, and B. Perers (2013). Short-term heat load forecasting for single family houses. *Energy and Buildings 65*, 101 – 112.

Bloess, A., W.-P. Schill, and A. Zerrahn (2018, February). Power-to-heat for renewable energy integration: A review of technologies, modeling approaches, and flexibility potentials. *Applied Energy 212*, 1611–1626.

Elci, M., B. M. Delgado, H.-M. Henning, G. P. Henze, and S. Herkel (2018). Aggregation of residential buildings for thermal building simulations on an urban district scale. *Sustainable Cities and Society 39*, 537 – 547.

EnergyPlus (2018). Weather Data by Location.

Evangelisti, L., C. Guattari, P. Gori, and F. Bianchi (2017). Heat transfer study of external convective and radiative coefficients for building applications. *Energy and Buildings 151*, 429 – 438.

Fonseca, J. A., T.-A. Nguyen, A. Schlueter, and F. Marechal (2016). City Energy Analyst (CEA): Integrated framework for analysis and optimization of building energy systems in neighborhoods and city districts. *Energy and Buildings 113*, 202–226.

Harish, V. and A. Kumar (2016). A review on modeling and simulation of building energy systems. *Renewable and Sustainable Energy Reviews 56*, 1272 – 1292.

Intergovernmental Panel on Climate Change (2018). Summary - Global Warming of 1.5 °C.

International Energy Agency (2018). Buildings.

IRENA (2018). Power system flexibility for the energy transition, Part 1: Overview for policy makers. pp. 48.

ISO 13790 (2008). ISO 13790:2008.

Ke, X., A. Jiang, and N. Lu (2016, July). Load profile analysis and short-term building load forecast for a university campus. In *2016 IEEE Power and Energy Society General Meeting (PESGM)*, pp. 1–5.

Meyabadi, A. and M. Deihimi (2017). A review of demand-side management: Reconsidering theoretical framework. *Renewable and Sustainable Energy Reviews 80*, 367 – 379.

Pajot, C., B. Delinchant, Y. Marechal, and D. Fresier (2018). Impact of Heat Pump Flexibility in a French Residential Eco-District. *Buildings 8*(10), 145.

Peuportier, B. and I. Blanc (1990). Simulation tool with its expert interface for the thermal design of multizone buildings. *International Journal of Solar Energy 8*(2), pages 109 – 120.

Reinhart, C. F. and C. C. Davila (2016). Urban building energy modeling a review of a nascent field. *Building and Environment 97*, 196 – 202.

Remmen, P., M. Lauster, M. Mans, M. Fuchs, T. Osterhage, and D. Mller (2018, January). TEASER: an open tool for urban energy modelling of building stocks. *Journal of Building Performance Simulation 11*(1), 84–98.

Yildiz, B., J. Bilbao, and A. Sproul (2017). A review and analysis of regression and machine learning models on commercial building electricity load forecasting. *Renewable and Sustainable Energy Reviews 73*, 1104 – 1122.